Dopamine-Derived Graphite-Like Hard Carbon Materials for High-Performance Li$^+$ Ions Storage

Xianfa Rao[1,2], Baobao Li[1,4], Kuang Lei[1], Yitao Lou[1,4], Lixia Zhang[1], Longhai Weng[1], Longxing Chen[1], Xuanbo Shi[1], Shengwen Zhong[1,‡], Bao Liu[3,‡] & Li Wang[4,‡]

[1] Faculty of Materials Metallurgy and Chemistry, Jiangxi University of Science and Technology, Ganzhou, Jiangxi, China

[2] Collaborative Innovation Center for Development and Utilization of Rare Metal Resources Co-sponsored by Ministry of Education and Jiangxi Province, Jiangxi University of Science and Technology, Ganzhou, Jiangxi, China

[3] Lanzhou Institute of Chemical Physics, Chinese Academy of Science, Laboratory of Clean Energy Chemistry and Materials, State Key Laboratory of Solid Lubrication, Lanzhou, Gansu, China

[4] School of Materials Science and Engineering, Luoyang Institute of Technology, Luoyang, Henan, China

Correspondence: Shengwen Zhong, Faculty of Materials Metallurgy and Chemistry, Jiangxi University of Science and Technology, Ganzhou, Jiangxi, 341000, China. Tel: 86-139-797-07564. E-mail: zhongsw-jxust@outlook.com

Bao Liu, Lanzhou Institute of Chemical Physics, Chinese Academy of Science, Laboratory of Clean Energy Chemistry and Materials, State Key Laboratory of Solid Lubrication, Lanzhou, Gansu, 730000, China. Tel: 86-173-615-52659. E-mail: liubao921@163.com

Li Wang, School of Materials Science and Engineering, Luoyang Institute of Technology, Luoyang, Henan, 471000, China. Tel: 86-137-216-75341. E-mail: 83362102@qq.com

‡ *These authors contributed equally to this manuscript.*

Abstract

Graphite anode material is easily powdered under large currents, resulting in a short circuit inside the battery, causing serious safety hazards. Therefore, it is necessary to study a negative electrode material, increase the diffusion channel of lithium ions, increase the layer spacing, reduce the transmission distance, effectively weaken the lithium-ion deposition, and improve the cycle life. A novel organic hard carbon material was prepared by calcining dopamine hydrochloride (DA) at three temperatures. Under the inert atmosphere of 950 °C, the material is fully carbonized, the lattice spacing is 0.367 nm, and it has good lithium-ion transmission activity. After assembling into a battery, after 2000 charge-discharge tests at a high rate of 10C, the charging specific capacity is still 103.3 mAh g-1, and the CE remains 101.4%. Dopamine hard carbon anode materials exhibit excellent specific capacity and cycle properties, providing new ideas to support the rapid charging and discharging of hard carbon anode materials.

1. Introduction

With the development and progress of human society, the global energy increasing nervous, and phase current as high energy consumption in our country, the main task of the development of new energy had become commercial lithium-ion batteries since the 1990s. Lithium-ion batteries (LIBs) have been widely used in mobile communications, information technology, medical equipment, and many other fields (Arora, White, & Doyle, 1998; Fan et al., 2018; F. Yang et al., 2011). In recent years, lithium-ion batteries have made some breakthroughs in the field of mobile vehicles, and fast-charging lithium-ion batteries have become an important research direction (Nitta & Yushin, 2014; Tirado, 2003). Lithium-ion battery is mainly composed of negative electrode, diaphragm, positive electrode, and electrolyte, among them, the anode material is an important guarantee for the electrochemical properties and safety of lithium-ion batteries under different working conditions. In the charging

process, lithium ions are released from the lattice of the positive active substance and embedded into the lattice of the negative active substance (Gibertini et al., 2021; Jing et al., 2021). When the lattice of the active substance embedded in the negative electrode is charged quickly, the concentration of lithium ions at the negative electrode increases rapidly under the support of large current, resulting in intensified polarization. The pressure of the negative electrode accepting lithium ions increases, which is easy to lead to structural collapse, capacity reducing, and even safety problems. Therefore, the solution to the problem of capacity maintenance during lithium-ion rapid charging lies the materials that can be allowed to rapid embedding of lithium ions in the negative electrode (Lu et al., 2015; Liu, Zhu, & Cui, 2019; Lee, 2021). Carbon material has the advantages of low-cost, low electrode potential and high capacity, preferred anode material to lithium-ion battery. Graphite not only has the advantages of high capacity (372 mAh g^{-1}) and low electrode potential (0.01 ~ 0.2V), but also relies on a good layered structure, which is conducive to the insertion and release of lithium ions. In addition, it has good chemical stability at room temperature and is resistant to corrosion by acids, alkalis, or organic solvents (Peng et al., 2017; Zhao et al., 2021; Gao et al., 2020). But the graphite layer structure determines the lithium ion can only from end face embedded, anisotropic leads to uneven lithium-ion diffusion path length, in addition, the specific surface area of graphite is a small, this site offers limited active point, lead to limited the amount of lithium ion embedded. Besides, the small interlayer spacing of graphite makes the diffusion resistance of lithium-ion intercalation high, leading to the rapid decay of graphite circulating capacity (Arora, White, & Doyle, 1998; Z. Wang, K., Wang et al., 2021). In particular, the large current of graphite under large polarization will make the potential of lithium embedding in graphite less than 0 V, and a large amount of deposition on the surface of graphite, resulting in the blockage of diffusion channel and the increase of resistance. As a result, the lithium source cannot be effectively utilized, the capacity attenuates, and the cycling performance declines sharply (Wang et al., 2021; Lin et al., 2013; Zhang et al., 2000). Graphite anode material is easy to pulverize under high current, which leads to short circuit inside the battery, causing serious safety risks. Therefore, it is necessary to study a cathode material to increase the diffusion channel of lithium ion, increase the layer spacing, reduce the transmission distance, effectively weaken the lithium deposition, and improve the cycle life. Hard carbon, known as no graphitized carbon material, is characterized by many randomly distributed sheets of bent graphite that cannot be reshaped into graphite at 3,000 ℃ or more. The non-graphitized nature of the hard carbon can be attributed to the formation of cross-linked or covalent C-O-C bonds in the precursor. The formation of rigid cross-linked structures in his precursors during pyrolysis, as well as defects, micropores and oxygen-containing functional groups, greatly inhibited the growth of graphite flakes. Even at high treatment temperatures, hard carbon forms only short-range orientation (Sun et al., 2019; Shen et al., 2018; Wu et al., 2019).

In this paper, a kind of hard carbon material with similar graphite layer structure was obtained by using dopamine as carbon source under high temperature carbonization. Its initial specific capacity is 342.7mAh g^{-1}, which is like graphite in capacity, but more outstanding in cycle and rate performance outstanding, providing a new idea for lithium-ion battery anode materials.

2. Experiment

2.1 Preparation of Hard Carbon Materials DA-800, DA-950 and DA-1100

Taking dopamine hydrochloride (DA) as a raw material, 10g dopamine hydrochloride were added to the porcelain boats, sealed, and then placed into the tube furnace with N_2 atmosphere in stages. The temperature was raised to 530 ℃ at the rate of 3 ℃/min, and the temperature was kept for 2 hours. After that, the temperature was raised to 800 ℃, 950 ℃ and 1100 ℃ at the rate of 2 ℃/min. Carbonize for 2 hours, then cool to room temperature. The preparation process is shown in Figure 1. The porcelain boat was removed to obtain fluffy and porous dopamine carbon material, and then the dopamine carbon material was ground and sieved (300 mesh) to obtain DA hard carbon powder, named DA-800, DA-950 and DA-1100, respectively.

2.2 Preparation of Electrode Sheet and Assembly of Battery

DA hard carbon, super P (SP) and polyvinylidene fluoride (PVDF) were mixed in a ratio of 8:1:1. The 5 g mixture was added to 40 mL N-methyl pyrrolidone (NMP) solvent. After ball milling for 12 h, the paste was evenly coated on the surface of copper foil and dried at 120 ℃ for 2 h. The dry film was cut into circular sheets with a diameter of 1.2 cm. The area mass load of the electrode were about 3.0 mg cm^{-2}. The cut discs are dried in a 60 ℃vacuum oven for 12 hours and then placed in a glove box with argon atmosphere to assemble the battery. A lithium-ion battery was assembled using a lithium sheet as a counter electrode, 1.2 g mL^{-1} $LiPF_6$ dissolved in a mixed carbonate solvent (EC/DEC=1:1) as electrolyte, and Celgard®3501(Calgary, LLC, Charlotte, USA) as diaphragm.

2.3 Characterization and Electrochemical Test

X-ray diffraction (XRD) spectra were collected by using copper Kα rays in brock powder X-ray diffractometer. Infrared spectrum (IR) was measured by Fourier transform infrared spectrophotometer BrukerIFS66/S. Raman spectra were measured using a thermal DXR micro laser Raman spectrometer. Scanning electron microscope (SEM) images was captured using a Zeiss 340 scanning electron microscope analyzer. TEM images were obtained

by TEITecnaiG2F20 transmission electron microscope. Before assessing electrochemical performance, all cells were pretreated and discharged from open circuit voltage (OCV) to 0.01V at a current of 0.1 mA and charged to 2.5 V at the same rate. The electrochemical performance of cells were evaluated using Abrin cell Test station (BT2000, Bing Instruments, USA). Cyclic voltammetry curves from 0.01 to 2.5 V were recorded at a rate of 0.1 mV s^{-1} using Solation 1260tron/1287 electrochemical interface (Mileages, UK). Impedance analysis was also performed using the Solatron126tron/1287 electrochemical interface kit.
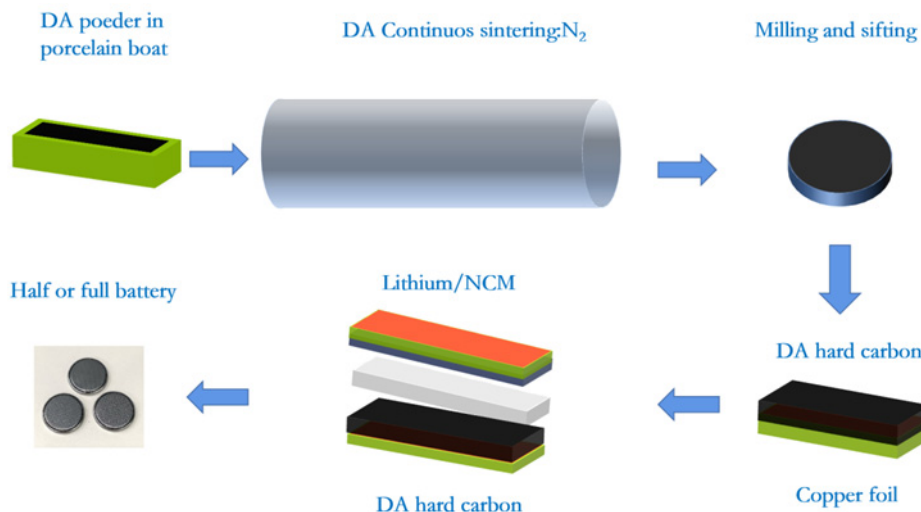

Figure 1. Preparation process of DA hard carbon material

3. Results and Discussion

3.1 Dopamine-Derived Hard Carbon Characterization Test
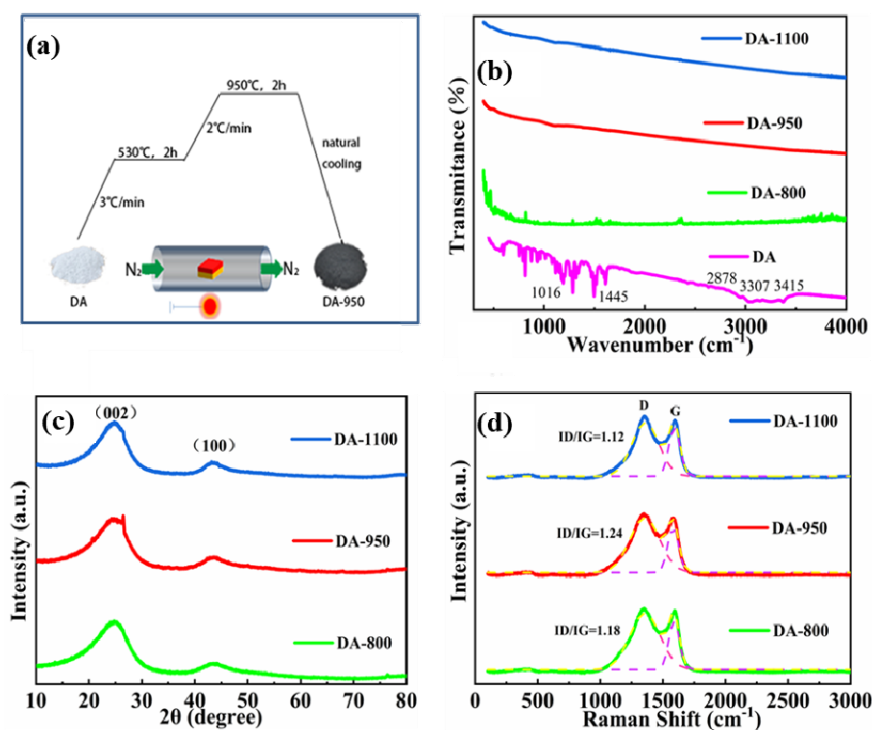

Figure 2. (a) Carbonization temperature control of DA-950 in nitrogen atmosphere; (b) Infrared spectra of the three samples; (c) XRD spectra of the three samples; (d) Raman spectra of the three samples

The heating entity diagram of DA-950 is shown in Figure 2(a). Infrared spectroscopy (Figure 2(b)) showed the presence of characteristic vibration peaks of uncarbonized dopamine hydrochloride at the C-N bond at 1016 cm^{-1}, sp^3 C-H bond at 2878 cm^{-1}, -N-H bond at 3307 cm^{-1}, -O-H bond at 3415 cm^{-1}, and benzene ring at 1300-1600 cm^{-1}. However, the characteristic vibration peaks of C-N bond, -N-H bond, -O-H bond and benzene ring completely disappear after carbonization at 800 °C, 950 °C and 1100 °C, respectively, indicating that DA is completely carbonized at these three temperatures, and organic hard carbon materials with high carbon content are obtained. The structures of DA at three temperatures were characterized by X-ray diffraction (XRD) and Raman spectroscopy (Raman). As shown in Figure 2(c, d), it is found that DA has two wide peaks around 25° and 43°, which are related to the (002) and (100) lattice planes of disordered carbon structure respectively. With the increase of carbonization temperature, the DA peak pattern does not change obviously, indicating that they are all hard carbons. However, at different carbonization temperatures, the peak of (002) has a slight angular shift, which implies a change in the distance between layers. According to Bragg equation, the values of DA-800, DA-950 and DA-1100 0.363, and 0.361 nm, respectively. Although there is a slight difference in the layer spacing, the d$_{002}$ value of the three temperatures are still much higher than that of graphite (0.335 nm), which can promote the electrochemical insertion and removal of Li$^+$, and is conducive to increase of the capacity. Especially under the support of high-rate current, the large layer spacing and disordered carbon structure can effectively deal with the plugging problem of Li$^+$ when inserting into the carbon layer, to improve the cycle stability and capacity retention rate of high-rate current. For Raman spectra of DA at different temperatures, as shown in Figure 2(d), there are two separation bands about 1357 cm^{-1} (D band) and 1589 cm^{-1} (G band), corresponding to disordered SP^3 hybrid carbon of carbon atom and graphite-like sp^2 hybrid carbon of ordered layered structure. It shows that DA after carbonization is composed of disordered SP^3 hybrid carbon and ordered graphite-like sp^2 hybrid carbon. In addition, the peak intensity ratio (I$_D$/I$_G$) of D-band and G-band indicates the degree of graphite ordering. The I$_D$/I$_G$ of DA-800, DA-950 and DA-1100 are 1.18, 1.24 and 1.12, respectively, and the area ratio is 3.21, 3.34 and 2.64, indicating that disordered SP^3 hybrid carbon is dominant. Compared with the other two temperatures, DA-950 has more disordered SP^3 hybrid carbon, and the more disordered structure can provide more Li$^+$ fast channels in the process of rapid charge and discharge. Moreover, the disordered structure can support each other and is not easy to collapse (Xie et al., 2021), which ensures the capacity increase and cycle stability of rapid charge and discharge.
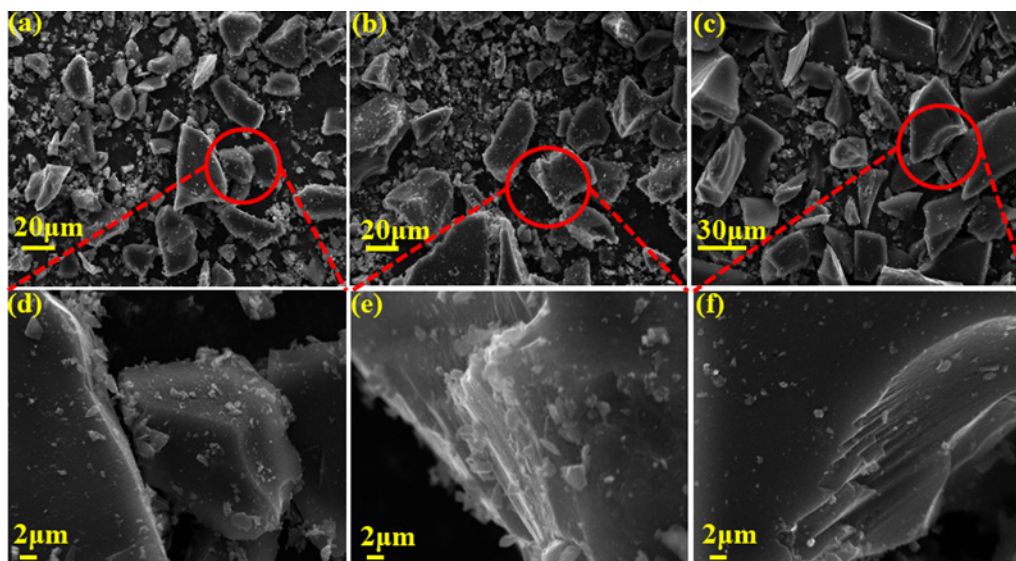

Figure 3. (a)(d) SEM image of DA-800; (b)(e) SEM image of DA-950; (c)(f) SEM image of DA-1100

Due to the grinding and screening of DA, DA at all three temperatures presents "frag-like distribution". The small particles have poor morphology uniformity, while the large particles are massive and have an ordered and compact layered structure, exposing more active sites, to maximize and effectively achieve the embedding and extrication of lithium ions. Due to the grinding and screening of DA, DA at all three temperatures presents "fragmentary distribution". As shown in Figure 3(a-c), small particles have poor morphology uniformity, while large particles have large volume and orderly and dense layered structure, exposing more active sites and maximizing and

effectively achieving lithium ion embedding and extraction. Further observation shows that da-950 exposes more defects on the surface than the other two particles, as shown in Figure 3(d-f), which is conducive to the embedding of Li^+ at the active point. To sum up, DA-950 has a layered structure just suitable for Li^+ embedding, which is conducive to the rapid transportation of Li^+ and makes it have outstanding performance in magnification performance.
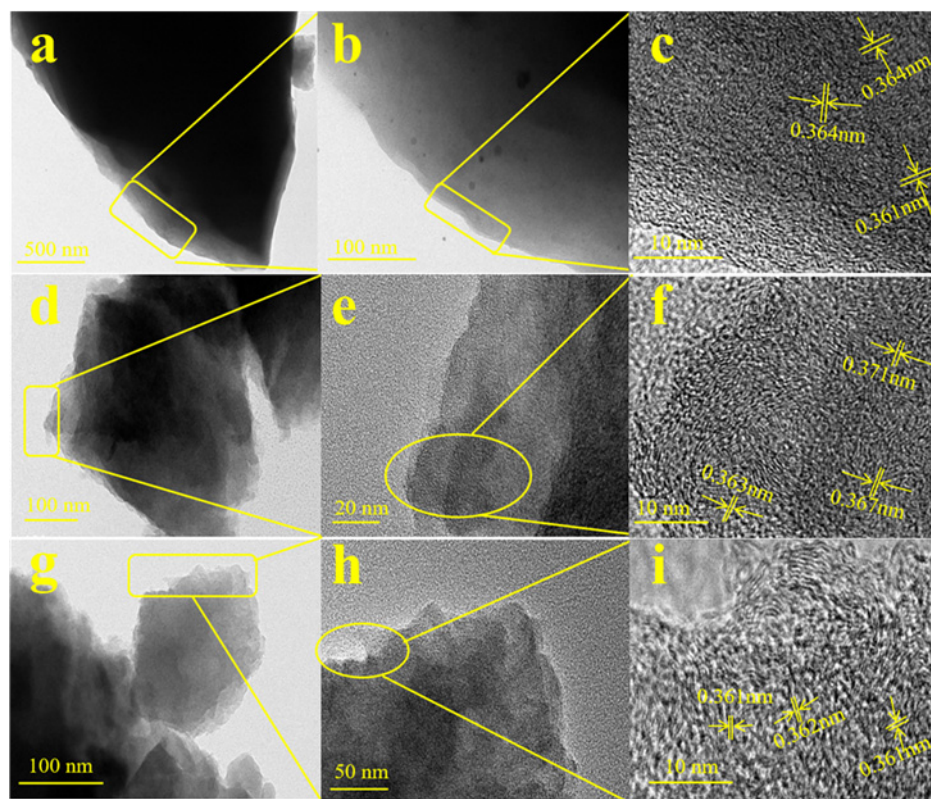

Figure 4. (a-c) TEM image of DA-800; (d-f) TEM image of DA-950; (g-i) TEM image of DA-1100

In order to further explore the differences in the microstructure of the three materials, TEM characterization was carried out for the three samples. As shown in Figure 4, the observed DA lattice fringes were staggered and confused, indicating the overlapping of the isolation layers and the disordered accumulation layer at the graphite carbon level, which is made up of ordered and disordered layered structure of amorphous carbon, and this structure can effectively solve the problem that graphite material lithium ion can only from the end of the embedded defects the carbon layers with different orientations make it easier to embedded and disembodying. Lithium ions dynamically, providing a superior transmission path and platform for Li^+, and shortening the transmission path to a certain extent, which is more conducive to the rapid embedding of Li^+. In addition, the lattice spacing of DA-950 is 0.367nm, which are better than that of DA-800 and DA-1100, and the layer spacing of the three samples is better than that of graphite, which is 0.335nm. This means that the three materials of DA will have a higher capacity and better rate performance.

3.2 Electrochemical Performance Test of Dopamine-Derived Hard Carbon
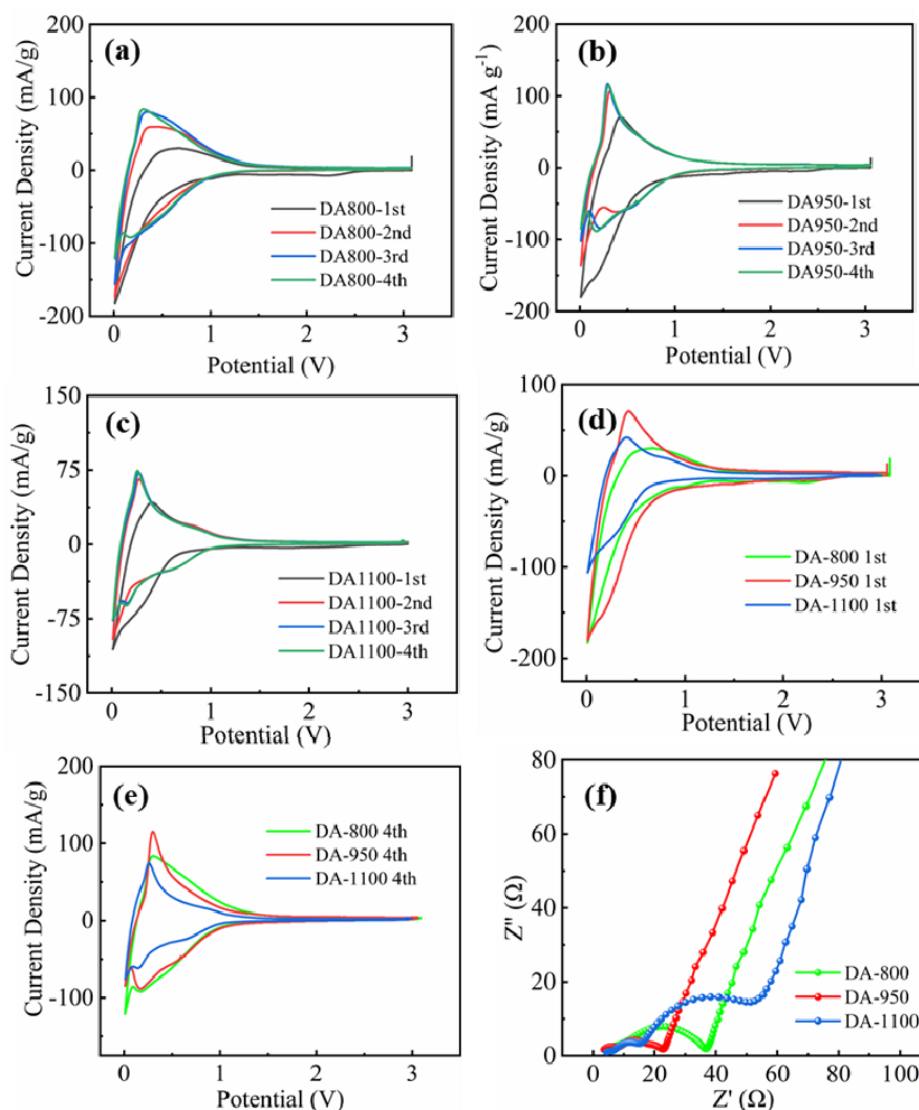
Figure 5. (a-c) are curves of voltametric characteristics of DA-800, DA-950 and DA-1100, respectively. (d) and (e) show the comparison of voltametric characteristic curves of the first and fourth cycles of three DA temperature gradients. (f) EIS impedance spectra of DA at three temperature gradients

In order to investigate the lithium storage performance of DA hard carbon materials, DA and Li metal were used as working electrode and opposite electrode to assemble buckle semi-battery. Figure 5(a-c) study the cyclic voltammetry curves (CV) of three temperature gradients DA. It can be observed that DA-800, DA-950 and DA-1100 all have two groups of REDOX peaks: strong peaks of DA-800 at 0.17V and 0.31V, strong peaks of DA-950 at 0.18V and 0.3V, and strong peaks of DA-1100 at 0.15V and 0.26V. All correspond to the peaks of the ordered graphite-like lamellar structure of lithium embedding and exhuming. In addition, the weak peaks of DA-800 at 0.61V and 0.82V, DA-950 at 0.60V and 0.85V, and DA-1100 at 0.76V and 0.89V correspond to the weak bulking peaks and DE lithium peaks of disordered hard carbon structure. The results showed that the CV curve is in good agreement with the microstructure of electrode material. XRD patterns and Raman spectra confirmed that DA samples were composed of ordered layered structures like graphite and amorphous structures with low crystallinity, corresponding to the REDOX peaks in CV curves of different morphologic structures. Therefore, the CV curves of the three DA gradients all showed a very high degree of overlap after the first cycle, indicating that DA has good stability in the cycle process and the specific capacity is not easy to decay. As shown in Figure 5(d) and (e), in the first and fourth circle CV diagrams, the three-temperature materials DA showed obvious REDOX peaks in the first circle, because the electrode materials need to be activated under the support of current. The cyclic voltammetry curves of the battery assembled by different electrode resistance were further

tested under different cycles. When the sweep speed was kept at 0.1mV s^{-1}, DA-950 had a larger circle area and specific capacity than the other two materials under the same current, and the capacity distribution was more extensive under 0~3V, as shown in Figure 5(d). After 4 cycles, the potential difference is reduced, the symmetry is better, and the irreversible capacity is reduced.，indicating that the specific capacity of the DA-950 has a higher specific capacity.

The electrode materials prepared at three temperatures were assembled into button cells, which were activated at a current density of 100 mA g^{-1} and tested for impedance, as shown in Figure 5(f). In the high frequency region, the inflection point value of the first semicircle is R$_{SEI}$ (interface layer resistance), and the inflection point value of the second semicircle is R$_{CT}$ (charge transfer resistance). The diagonal line in the low-frequency region is the Warburg impedance (W1), representing the diffusion resistance of lithium ions in the electrode sheet. The results show that DA-950 exhibits smaller R$_s$ and R$_{ct}$ in the high frequency region and smaller Warburg impedance in the low frequency region, which is more favorable for lithium-ion transport. This is due to the larger lattice stripes of DA-950 and the greater performance of disordered sp^3 hybrid carbon compared to DA-800 and DA-1100.
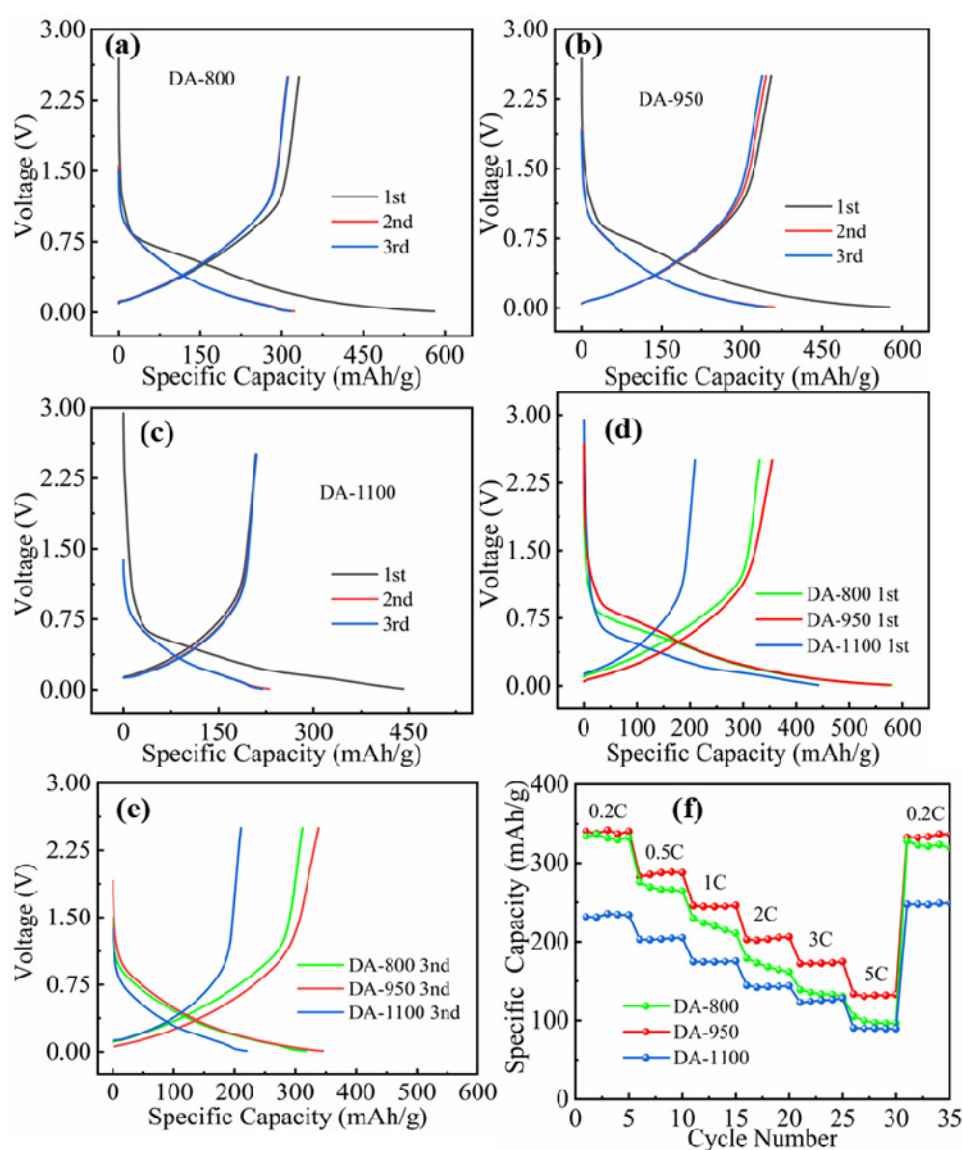

Figure 6. (a) Charge and discharge curves of DA-800; (b) The charge-discharge curve of DA-950; (c) Charge-discharge curve of DA-1100; (d) Comparison of initial charge-discharge curves of DA-800, DA-950 and DA-1100; (e) Comparison of the third charge and discharge curves of DA-800, DA-950 and DA-1100; (f) Rate performance of DA-800, DA-950 and DA-1100

Figure 6(a-c) shows the constant current charge and discharge of DA materials at three temperatures. Can be observed that under 0.1 V platform related with the proportion of the total discharge capacity decreases with the increase of cycling times, due to the electrolyte can infiltrate into pores, can effectively reduce the Li^+ ion diffusion distance, led to a huge surface area of electrode/electrolyte interface, big enough to absorb the Li^+ ions, promote fast charge transfer reaction. The voltage platform of DA electrode consists of two stages, the charge and discharge process between 0.5~1.0V determined by the amorphous structure and the charge and discharge process between 0.01~0.5V determined by the ordered graphite-like structure. Comparing the first and third charge-discharge curves of DA-800, DA-950 and DA-1100, as shown in Figure 6(d, e). The initial charging specific capacities of DA-800, DA-950 and DA-1100 are 331.0 mAh g^{-1}, 354.4 mAh g^{-1}, 441.8mAh g^{-1}, respectively, and the Coulomb efficiencies are 57.1%, 61.6% and 47.1%. The DA-950 has high specific charge capacity and high charge and discharge efficiency. As reflected by Raman curves and TEM images, DA-950, a material with stronger disorder, not only has the best diffusion channels for lithium ions, but also has abundant active sites. Figure 6(f) compares the rate performance of DA-800, DA-950 and DA-1100. At 0.2C, 0.5C, 1C, 2C, 3C and 5C, the DA-950 shows superior magnification performance, especially at large magnification. In addition, when it restored to 0.2c, the capacity of DA electrode recovers rapidly, which shows that DA has strong adaptability in changing current density and its structure is stable and not easy to collapse.
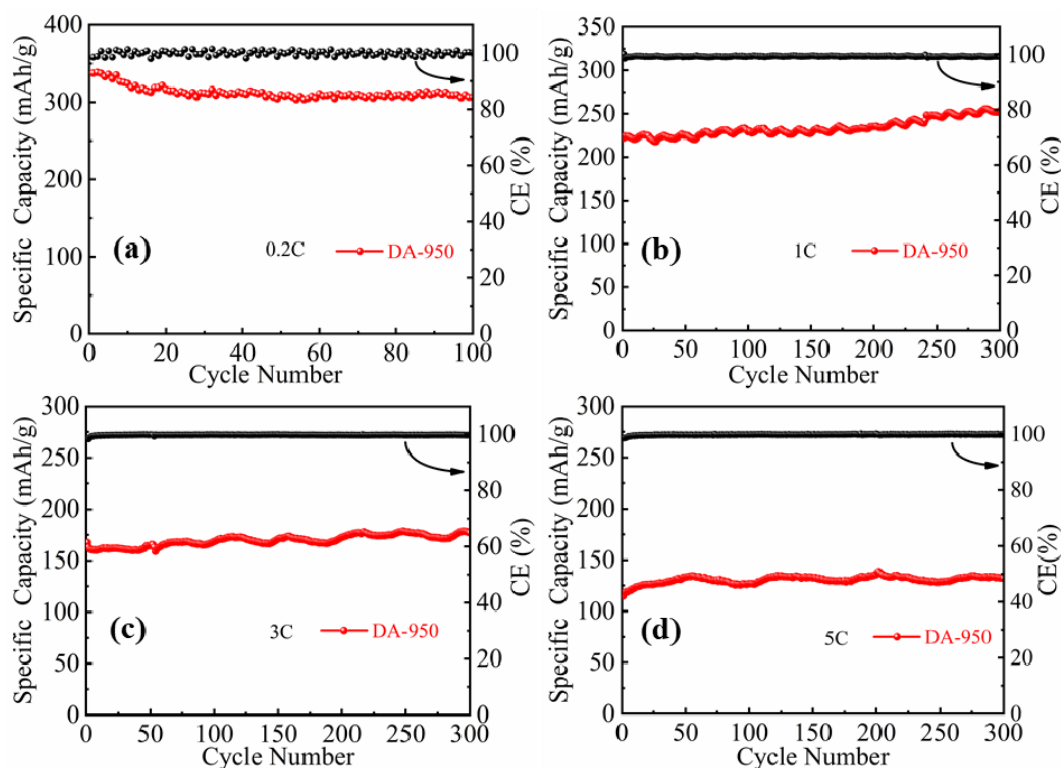

Figure 7(a-d). The cyclic curves of DA-950 at 0.2C, 1C, 3C and 5C

In order to evaluate the long-term cycle stability of DA anode materials at different rates, DA-950, which is superior in all aspects, is selected for long cycle at 0.2C, 1C, 3C and 5C rates, as shown in Figure 7(a-d). Further long cycle tests were carried out on da-950 battery samples at different rates. The results showed that the specific capacity of first charge at 0.2c rate was 337.5 mAh g^{-1}, and the specific capacity of charge after 100 cycles was 306.5 mAh g^{-1}, and the capacity retention rate was 89.44%. After 300 cycles of constant current charge-discharge tests at 1C and 3C rates, the capacity retention rates are 103.9%h and 114.1%, respectively. When upgraded to 5C, the specific charging capacity still has 132.2 mAh g^{-1} and coulomb efficiency reaches 115.2% after 300 turns. The results show that DA-950 has good cyclic stability in the cycle process, and the specific charging capacity of DA-950 will rise slightly in the process of high-power cycle. This is because under the loading of high-power current, more active points will be excited and more Li^+ will be embedded, thus increasing the capacity.

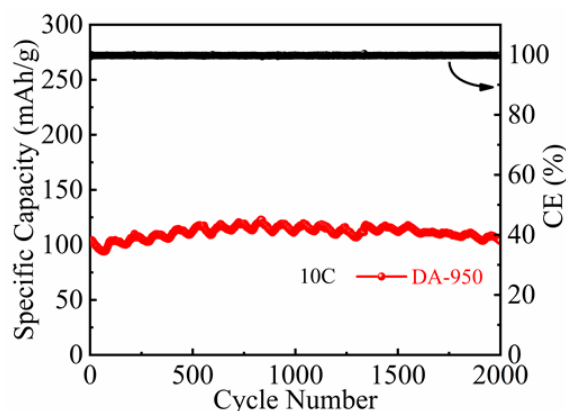Figure 8. The cycle curve of DA-950at10Csuper-magnification current

The cyclic performance and stability of DA-950 under ultra-large rate current were investigated (Figure 8). DA-950 has a specific capacity of 101.9 mAh g^{-1} at the first charge at the high rate of 10C and 103.3 mAh g^{-1} after 2000 cycles, with a retention rate of 101.4%. The results show that the structure of DA-950 is stable without the phenomenon of structural collapse under the addition of 10C super-large multiplier, and it can still stimulate more active sites, and the capacity also shows a wave trend of small increase.

The excellent lithium-ion transport properties of dopamine hard carbon materials are attributed to the synergistic effect of the short-range ordered and long-range disordered amorphous carbon structure and the graphitic layered structure, and the edge defects are the insertion and extraction of lithium ions. Although direct carbonization of dopamine as an anode material for Li-ion batteries is rarely reported, dopamine, as an endogenous nitrogen-containing organic compound, can be used as nitrogen-doped carbon sheets as energy storage materials. Li et al. used dopamine-derived nitrogen-doped carbon sheets as an anode material for high-performance sodium-ion batteries (Z. Yang et al., 2015), it has excellent cycling stability at a current density of 200 mA g^{-1} (165 mAh g^{-1}, without any decay after 600 cycles); In addition, polydopamine (PDA) nanofilms can polymerize and form polydopamine (PDA) nanofilms on almost any solid surface when exposed to air under weak alkaline conditions (pH 8.5), and this property is often used as a material coating. In 2018, WU et al. used polydopamine to coat square ferric oxide, followed by calcination in an argon atmosphere to obtain carbon-coated ferric oxide (Q. Wang, B. Wang, et al., 2018). The thickness of the carbon layer converted by polydopamine coating is 20–40 nm, but the overall cost is relatively expensive.

4. Conclusions

A kind of carbon material with graphite layer structure is obtained by carbonizing dopamine HCl (DA) at high temperature. The carbon structure is the combination of disordered SP^3 hybrid carbon and ordered sp^2 hybrid carbon, showing the mixed channel structure of long-range disorder and short-range order. Compared with DA-800 and DA-1100, DA-950 has a larger lattice spacing, a more chaotic carbon structure, a larger CV curve shape and a smaller R_{SEI}, R_{CT} and Warburg impedance. The DA-950 anode material is more excellent in rate performance and cycle stability. At the super-large rate of 10C, after 2000 cycles, the specific charging capacity is 103.3mAh g^{-1}, and the retention rate is 101.4%. The DA-950 shows great potential for commercial applications, and this work could advance the development of low-cost and sustainable carbon materials.

5. Acknowledgments

References

Arora, P., White, R. E., & Doyle, M. (1998). Capacity fade mechanisms and side reactions in lithium-ion batteries. *Journal of the Electrochemical Society*, *145*(10), 3647. https://doi.org/10.1149/1.1838857

Fan, X., Sun, W., Meng, F., Xing, A., & Liu, J. (2018). Advanced chemical strategies for lithium–sulfur batteries: A review. *Green Energy & Environment*, *3*(1), 2-19. https://doi.org/10.1016/j.gee.2017.08.002

Gao, S., Jiang, Q., Shi, Y., Kim, H., Busnaina, A., Jung, H. Y., & Jung, Y. J. (2020). High-performance lithium battery driven by hybrid lithium storage mechanism in 3D architectured carbonized eggshell membrane anode. *Carbon*, *166*, 26-35. https://doi.org/10.1016/j.carbon.2020.05.006

Gibertini, E., Liberale, F., Dossi, C., Binda, G., Mattioli, B., Bettinetti, R., ... & Magagnin, L. (2021). Algae-derived hard carbon anodes for Na-ion batteries. *Journal of Applied Electrochemistry*, *51*(12), 1665-1673. https://doi.org/10.1007/s10800-021-01609-2

Jing, W., Wang, M., Li, Y., Li, H. R., Zhang, H., Hu, S., ... & He, Y. B. (2021). Pore structure engineering of wood-derived hard carbon enables their high-capacity and cycle-stable sodium storage properties. *Electrochimica Acta*, *391*, 139000. https://doi.org/10.1016/j.electacta.2021.139000

Lee, Y. K. (2021). Effect of transition metal ions on solid electrolyte interphase layer on the graphite electrode in lithium ion battery. *Journal of Power Sources*, *484*, 229270. https://doi.org/10.1016/j.jpowsour.2020.229270

Lin, X., Park, J., Liu, L., Lee, Y., Sastry, A. M., & Lu, W. (2013). A comprehensive capacity fade model and analysis for Li-ion batteries. *Journal of The Electrochemical Society*, *160*(10), A1701. https://doi.org/10.1149/2.040310jes

Liu, Y., Zhu, Y., & Cui, Y. (2019). Challenges and opportunities towards fast-charging battery materials. *Nature Energy*, *4*(7), 540-550. https://doi.org/10.1038/s41560-019-0405-3

Lu, D., Shao, Y., Lozano, T., Bennett, W. D., Graff, G. L., Polzin, B., ... & Xiao, J. (2015). Failure mechanism for fast-charged lithium metal batteries with liquid electrolytes. *Advanced Energy Materials*, *5*(3), 1400993. https://doi.org/10.1002/aenm.201400993

Nitta, N., & Yushin, G. (2014). High-capacity anode materials for lithium-ion batteries: choice of elements and structures for active particles. *Particle & Particle Systems Characterization*, *31*(3), 317-336. https://doi.org/10.1002/ppsc.201300231

Peng, H. J., Huang, J. Q., Cheng, X. B., & Zhang, Q. (2017). Review on high-loading and high-energy lithium–sulfur batteries. *Advanced Energy Materials*, *7*(24), 1700260. https://doi.org/10.1002/aenm.201700260

Shen, C., Hu, G., Cheong, L. Z., Huang, S., Zhang, J. G., & Wang, D. (2018). Direct Observation of the Growth of Lithium Dendrites on Graphite Anodes by Operando EC-AFM. *Small Methods*, *2*(2), 1700298. https://doi.org/10.1002/smtd.201700298

Sun, Y., Wang, L., Li, Y., Li, Y., Lee, H. R., Pei, A., ... & Cui, Y. (2019). Design of red phosphorus nanostructured electrode for fast-charging lithium-ion batteries with high energy density. *Joule*, *3*(4), 1080-1093. https://doi.org/10.1016/j.joule.2019.01.017

Tirado, J. L. (2003). Inorganic materials for the negative electrode of lithium-ion batteries: state-of-the-art and future prospects. *Materials Science and Engineering: R: Reports*, *40*(3), 103-136. https://doi.org/10.1016/S0927-796X(02)00125-0

Wang, B., Le Fevre, L. W., Brookfield, A., McInnes, E. J., & Dryfe, R. A. (2021). Resolution of Lithium Deposition versus Intercalation of Graphite Anodes in Lithium Ion Batteries: An In Situ Electron Paramagnetic Resonance Study. *Angewandte Chemie International Edition*, *60*(40), 21860-21867. https://doi.org/10.1002/anie.202106178

Wang, Q., Wang, B., Zhang, Z., Zhang, Y., Peng, J., Zhang, Y., & Wu, H. (2018). Tailoring yolk–shell FeP@ carbon nanoboxes with engineered void space for pseudocapacitance-boosted lithium storage. *Inorganic Chemistry Frontiers*, *5*(10), 2605-2614. http://doi.org.https.tsg.proxy.jxust.edu.cn/10.1039/c8qi00849c

Wang, Z., Wang, K., Gao, F., & Li, J. (2021). The investigation on degeneration mechanism and thermal stability of graphite negative electrode in lithium ion batteries from electric logistics vehicles. *Ionics*, *27*(1), 85-95. https://doi.org/10.1007/s11581-020-03804-1

Wu, X., Chen, Y., Xing, Z., Lam, C. W. K., Pang, S. S., Zhang, W., & Ju, Z. (2019). Advanced carbon-based anodes for potassium-ion batteries. *Advanced Energy Materials*, *9*(21), 1900343. https://doi.org/10.1002/aenm.201900343

Xie, L., Tang, C., Bi, Z., Song, M., Fan, Y., Yan, C., ... & Chen, C. (2021). Hard Carbon Anodes for Next-Generation Li-Ion Batteries: Review and Perspective. *Advanced Energy Materials*, *11*(38), 2101650. https://doi.org/10.1002/aenm.202101650

Yang, F., Zhang, Z., Du, K., Zhao, X., Chen, W., Lai, Y., & Li, J. (2015). Dopamine derived nitrogen-doped carbon sheets as anode materials for high-performance sodium ion batteries. *Carbon*, *91*, 88-95. https://doi.org/10.1016/j.carbon.2015.04.049

Yang, Z., Zhang, J., Kintner-Meyer, M. C., Lu, X., Choi, D., Lemmon, J. P., & Liu, J. (2011). Electrochemical energy storage for green grid. *Chemical reviews*, *111*(5), 3577-3613. https://doi.org/10.1021/cr100290v

Zhang, D., Haran, B. S., Durairajan, A., White, R. E., Podrazhansky, Y., & Popov, B. N. (2000). Studies on capacity fade of lithium-ion batteries. *Journal of Power Sources*, *91*(2), 122-129. https://doi.org/10.1016/S0378-7753(00)00469-9

Zhao, L. F., Hu, Z., Lai, W. H., Tao, Y., Peng, J., Miao, Z. C., ... & Dou, S. X. (2021). Hard carbon anodes: fundamental understanding and commercial perspectives for Na-ion batteries beyond Li-ion and K-ion counterparts. *Advanced Energy Materials*, *11*(1), 2002704. https://doi.org/10.1002/aenm.202002704